Journal of Quantitative Spectroscopy & Radiative Transfer 331 (2025) 109254

Contents lists available at ScienceDirect

Journal of Quantitative Spectroscopy and Radiative Transfer

journal homepage: www.elsevier.com/locate/jqsrt

# A mixing rule for imaginary parts of refractive indices of aerosols or colloids in the Rayleigh regime

Hans Moosmüller [a,*], Justin B. Maughan [b,c], Prakash Gautam [a], Christopher M. Sorensen [c]

[a] Laboratory for Aerosol Science, Spectroscopy, and Optics, Desert Research Institute, 2215 Raggio Parkway, Reno, NV 89512, USA
[b] Pratt Community College, 348 NE SR 61, Pratt, KS 67124, USA
[c] Department of Physics, Kansas State University, 116 Cardwell Hall, 1228 N. 17th Street, Manhattan, KS 66506, USA

ARTICLE INFO

*Keywords:*
Aerosols
Colloids
Complex refractive index
Mixing rules
Rayleigh regime
Effective medium theory

ABSTRACT

A Rayleigh mixing rule that relates the effective imaginary part of the refractive index of a composite medium, such as an aerosol or colloid, to the complex refractive index of the Rayleigh particles is derived using Rayleigh scattering theory. The derivation is simple, straightforward, and only weakly dependent on particle morphology. The Rayleigh mixing rule offers an opportunity to derive the imaginary part of refractive index spectra of Rayleigh particles, suspended in a non-absorbing medium with known refractive index spectrum, from an extinction spectrum of the composite medium. However, for this application, the real refractive index spectrum of the particle must be known reasonably well and the imaginary part must be known well enough to decide between two mathematical solutions for it. The Rayleigh mixing rule is compared with widely used mixing rules (i.e., volume, Maxwell Garnett, and Bruggeman mixing rules) and we show that in the small volume fraction regime both the Maxwell Garnet and Bruggeman mixing rules agree with the Rayleigh mixing rule.

## 1. Introduction

If small (compared to wavelength), absorbing particles are suspended dilutely in a non-absorbing medium (gas or liquid), a relationship is needed to relate the imaginary part of the particle refractive index to the bulk absorption coefficient of the composite medium. The term "composite medium" is used here to refer to the aerosol or colloid. Such a relationship can be used to directly relate the effective imaginary part of the refractive index or bulk absorption coefficient of the composite medium to the volume fraction and complex refractive index of the suspended particles. Obvious choices for such a relationship are various effective medium theories and their mixing rules (nicely summarized and tested by Chýlek et al. [1]). Here, we use Rayleigh scattering theory for a simple derivation of a mixing rule that achieves this goal. We compare this Rayleigh mixing rule with some common existing mixing rules.

The Rayleigh mixing rule can also be used to address the inverse problem of deriving the imaginary part of the particle refractive index from the absorption coefficient of the composite medium. This is quite useful because in the Rayleigh regime, where scattering is negligible, the absorption coefficient of a colloid can readily be measured as function of wavelength over the solar spectral range with a spectroradiometer. In addition, a wide variety of nanoparticles have recently become commercially available and colloids of such nanoparticles can be used for determining the imaginary part of the refractive index for the material that the nanoparticles consist of, generally only weakly dependent on particle shape.

## 2. Absorption in the Rayleigh regime

Consider a system of homogeneous, spherical particles suspended in a non-absorbing medium. In the medium, their relative refractive index $m$ is the ratio of their complex refractive index $m_0$ and the real refractive index $n_m$ of the surrounding medium [2,3], hence

$$m = n + i\,\kappa = \frac{m_0}{n_m} = \frac{n_0}{n_m} + i\,\frac{\kappa_0}{n_m}. \tag{1}$$

In Eq. (1), $i = \sqrt{-1}$ is the imaginary unit number and $n$ and $\kappa$ are the real and imaginary parts of the relative particle refractive index, respectively. Using these refractive indices, the particle optical properties in the medium can be calculated using the particle size parameter $x$ as

* Corresponding author.
*E-mail addresses:* Hans.Moosmuller@dri.edu (H. Moosmüller), justinm@prattcc.edu, maughan@phys.ksu.edu (J.B. Maughan), Prakash.Gautam@dri.edu (P. Gautam), sor@phys.ksu.edu (C.M. Sorensen).

https://doi.org/10.1016/j.jqsrt.2024.109254
Received 29 May 2024; Received in revised form 26 September 2024; Accepted 28 October 2024
Available online 7 November 2024

$$x = \frac{2\pi r}{\lambda}, \tag{2}$$

where $r$ is the particle radius and $\lambda$ the wavelength of the light in the surrounding medium, that is the vacuum wavelength divided by the refractive index of the medium with $\lambda = \lambda_{vac}/n_m$. For non-spherical particles, an effective radius $r_e$ ($r_e = 0.75\ V_{sp}/A$, where $V_{sp}$ is the volume of a single particle and $A$ is its projected area averaged over random orientations) is best used to calculate the size parameter [4]. Note that for aerosols, the surrounding medium is often standard air with $n_m = n_{air} = 1.0003 \approx 1$ in the visible [5], and then the particle refractive index $m_0$ and the vacuum wavelength $\lambda_{vac}$ can often be used directly. However, for colloids suspended in liquid media, the refractive index of the liquid $n_m$ in the visible may be substantially higher than 1, for example $n_m = n_{water} \approx 1.3$ for liquid water [6], or as high as $n_m \approx 1.9$ as useful for index matching with sapphire optics [7].

In the small particle or Rayleigh limit ($x \ll 1 and kx \ll 1$), Rayleigh theory gives a simpler and more easily understandable description of particle optics than Mie theory [8–12]. Rayleigh theory uses the Lorentz-Lorenz factor $LL(m)$ [13,14] expressed elegantly in terms of the relative complex refractive index $m$ as

$$LL(m) = \frac{m^2 - 1}{m^2 + 2}, \tag{3a}$$

or more complicatedly as function of the real and imaginary components $n$ and $\kappa$ of the relative complex refractive index $m$ (Eq. 1) as

$$LL(n,\kappa) = \frac{n^2 - \kappa^2 - 2 + (n^2 + \kappa^2)^2 + i\ 6n\kappa}{(n^2 - \kappa^2 + 2)^2 + 4n^2\kappa^2}. \tag{3b}$$

The imaginary part of $LL(m)$ (i.e., $Im[LL(m)]$) is conventionally denoted as $E(m)$ [10,15,16] and can be written as

$$E(m) = Im[LL(m)] = \frac{6n\kappa}{(n^2 - \kappa^2 + 2)^2 + 4n^2\kappa^2} = \frac{2}{3}\kappa\ \xi(m), \tag{4a}$$

where $\xi(m)$, a function of the relative complex refractive index $m$, was previously defined as [17,18]

$$\xi(m) = \frac{9n}{(n^2 - \kappa^2 + 2)^2 + 4n^2\kappa^2}. \tag{4b}$$

The Rayleigh particle absorption efficiency $Q_{abs\_Ray}$ (ratio of absorption cross-section to geometric cross-section) for spherical particles can be written simply as [10]

$$Q_{abs\_Ray}(x,m) = 4xE(m), \tag{5a}$$

yielding the Rayleigh absorption cross-section $C_{abs\_Ray}$ [19] as

$$C_{abs\_Ray}(x,m) = \frac{6\pi}{\lambda}V_{sp}\ E(m) = \frac{4\pi}{\lambda}V_{sp}\ \kappa\ \xi(m), \tag{5b}$$

where $V_{sp}$ is the volume of a single particle. Eq. (5b) illustrates that a linear dependence of the Rayleigh absorption cross section on the imaginary part of the refractive index κ, as perhaps expected intuitively, is modified by the function $\xi(m)$; this is the utility of $\xi(m)$.

Following Eq. (5b), the bulk Rayleigh absorption coefficient $\beta_{abs\_Ray}$ of a composite medium with a particle number density $N/V$ ($N$ absorbing particles per volume $V$) in a non-absorbing medium [19] becomes

$$\beta_{abs\_Ray}(x,m) = \frac{N}{V}\ C_{abs\_Ray}(x,m) = \frac{N}{V}\ \frac{6\pi}{\lambda}\ V_{sp}E(m) = \frac{N}{V}\frac{4\pi}{\lambda}V_{sp}\ \kappa\ \xi(m). \tag{6a}$$

Note that $\beta_{abs\_Ray}(x,m)$ has units of inverse length, hence its inverse can be thought of as a photon mean free path. Using the total particle volume $V_{tp} = NV_{sp}$ suspended in the volume $V$ and the particle volume fraction $f_v = V_{tp}/V$ yields

$$\beta_{abs\_Ray}(m) = \frac{6\pi}{\lambda}\frac{N\ V_{sp}}{V}E(m) = \frac{6\pi}{\lambda}\frac{V_{tp}}{V}E(m) = \frac{6\pi}{\lambda_{vac}}f_V n_m E(m), \tag{6b}$$

using the relationship $\lambda = \lambda_{vac}/n_m$ for the final result of Eq. (6b). Eq. (6b) gives the bulk Rayleigh absorption coefficient of the composite medium as a simple function of the particle volume fraction $f_v$, the refractive index $n_m$ of the non-absorbing medium, and the imaginary part $E(m)$ of the Lorentz-Lorenz factor $LL(m)$. Note that there is no explicit dependence of the absorption coefficient on particle size within the Rayleigh regime, just on *total particle volume* $V_{tp}$, because for $\kappa x \lesssim 0.1$ light fully penetrates particles and consequently particles act as volume absorbers [9,20].

## 3. Rayleigh mixing rule for small absorbing particles suspended in a non-absorbing medium

The absorption coefficient $\beta_{abs}$ of a bulk medium with the complex refractive index $m$ directly relates to the imaginary part $\kappa$ of its refractive index as [8,11]

$$\beta_{abs}(m) = \frac{4\pi}{\lambda_{vac}}\ \kappa\ . \tag{7}$$

We invert Eq. (7) to write the imaginary part of the effective refractive index of the composite medium $\kappa_{eff\_Ray}$ as function of the Rayleigh absorption coefficient $\beta_{abs\_Ray}$ of this medium as

$$\kappa_{eff\_Ray}(m) = \frac{\lambda_{vac}}{4\pi}\beta_{abs\_Ray}(m). \tag{8a}$$

We further use Eq. (8a) and Eq. (6b) to obtain

$$\kappa_{eff\_Ray}(m) = \frac{3}{2}f_V n_m E(m) = f_V n_m \kappa\ \xi(m) = f_V n_m \kappa \frac{9n}{(n^2 - \kappa^2 + 2)^2 + 4n^2\kappa^2}, \tag{8b}$$

and replacing the imaginary part of the refractive index of the particle in the medium $\kappa$ with $\kappa_0/n_m$ (see Eq. 1) yielding

$$\kappa_{eff\_Ray}(m) = f_V\kappa_0\ \xi(m) = f_V\kappa_0\frac{9n}{(n^2 - \kappa^2 + 2)^2 + 4n^2\kappa^2}. \tag{8c}$$

This simple equation is our Rayleigh mixing rule giving the effective imaginary part of the refractive index of the composite medium $\kappa_{eff\_Ray}$ as the product of the particle volume fraction $f_v$, the imaginary part of the particle refractive index $\kappa_0$, and the function $\xi(m)$ of the complex refractive index $m$ of the particle in the medium. With the exception of the function $\xi(m)$, the Rayleigh mixing rule is identical to the volume mixing rule [1] and therefore, we further discuss $\xi(m)$ in complex refractive index space below.

Also note that Eq. (8c) can be written as quadratic equation

$$\kappa^4 + \kappa^2(2n^2 - 4) - \kappa\frac{9nf_V n_m}{\kappa_{eff\_Ray}} + (n^2 + 2)\ = 0\ . \tag{8d}$$

and Eqs. (8c) and (8d) have the same four analytical solutions for $\kappa = \kappa_0/n_m$, two of which are real with physical meaning (see Section 3.1 *Use of Rayleigh mixing rule to determine the imaginary refractive index of particles*).

A contour plot of the function $\xi(m)$ of Eq. (8c) as function of the real and imaginary parts of the relative refractive index $m$, $n$ and $\kappa$, respectively, of the particles in the medium, is shown in Fig. 1. Within the range of Fig. 1 (i.e., $1 \le n \le 4$ and $0 \le \kappa \le 3$), the maximum of $\xi$ is $\xi_{max} = \xi(n = 1, \kappa = 1) = 1.125$ and the minimum of $\xi$ is $\xi_{min} = \xi(n = 4, \kappa = 3) \approx 0.0548$. This corresponds to a range of $\xi(m)$ of more than a factor of 20 within the plot range of Fig. 1. The contour lines in Fig. 1 are vertical for $\kappa = 0$, indicating that $\xi(m)$ is independent of $\kappa$ for $\kappa \approx 0$. For relatively small $n$ (i.e., $1 \le n \le 1.27$) and a relatively wide range of $\kappa$ (i.e., $0 \le \kappa \le 1$), the function $\xi(m)$ remains within 12.5% of 1 (i.e., $0.875 \le \xi(m) \le 1.125$) and the factor $\xi(m)$ can sometimes be neglected within this

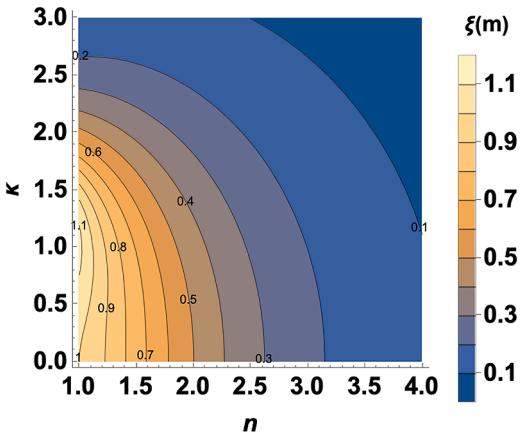


**Fig. 1.** Contour plot of the function $\xi(m)$ as function of the real and imaginary parts of the refractive index of the particle in the medium, $n$ and $\kappa$, respectively.

regime. However, for the largest relative refractive indices shown in Fig. 1, this factor becomes very important (i.e., $\xi(n = 4, \kappa = 3) \approx 0.0548$). Even larger refractive indices have been reported for metals at longer wavelengths, yielding even smaller values for $\xi(m)$. Recall from Eq.1 that relative refractive indices for the particles in the medium (i.e., $m$, $n$, $\kappa$) used here are the particle refractive indices (i.e., $m_0$, $n_0$, $\kappa_0$) divided by the real refractive index $n_m$ of the surrounding, non-absorbing medium.

Fig. 2 shows a log-log plot that demonstrates the functionality of $\kappa_{eff\_Ray}$ as a function of the imaginary part of the relative refractive index κ, for set values of the real part $n = 1.0, 2.0, 3.0, 4.0$. Fig. 2 essentially shows log-log x-y plots along four vertical lines (for the four set values of $n$) through the contour plot shown in Fig. 1.

For small $\kappa$ (i.e., $\kappa \ll 1$ and $\kappa \ll n$), it can be seen in Fig. 2 that $\kappa_{eff\_Ray}$ can be approximated as

$$\kappa_{eff\_Ray}(m) \approx f_v n_m \frac{9n}{(n^2+2)^2}\kappa = f_v \frac{9n}{(n^2+2)^2}\kappa_0, \quad \kappa \ll 1 \text{ and } \kappa \ll n, \tag{9}$$

which can easily be obtained by dropping the $\kappa^2$ and $\kappa^4$ terms from the denominator of Eqs. (8b, 8c), corresponding to $\xi_{small\_K}(m) = \frac{9n}{(n^2+2)^2}$ independent of $\kappa$. Eq. (9) still resembles the volume mixing rule with an additional, but simplified (compared to $\xi(m)$ in Eqs. 8) modifying factor of $\xi_{small\_K}(m) = \frac{9n}{(n^2+2)^2}$. In Fig. 2 it can be seen that $\kappa_{eff\_Ray}$ follows Eq. (9) to $\kappa \approx 0.8$, including the range of $\kappa$ found for most dominant components of atmospheric aerosols in the visible spectrum, with the possible exceptions of black carbon and hematite [21,22].

For large $\kappa$ (i.e., $\kappa \gg 1$ and $\kappa \gg n$), the dominant term in the denominator of Eq. (8c) is $\kappa^4$, and thus $\kappa_{eff\_Ray}$ limits to

$$\kappa_{eff\_Ray}(m) \approx 9 n_m f_v n \kappa^{-3} = 9 n_0 \, f_v \frac{n_m^3}{\kappa_0^3}, \quad \kappa \gg 1 \text{ and } \kappa \gg n, \tag{10}$$

corresponding to $\xi_{large\_K}(m) = \frac{9n}{\kappa^4}$. Fig. 2 shows that $\kappa_{eff\_Ray}$ follows Eq. (10) starting at $\kappa \approx 10$. There is a cross over region between $\kappa \approx 0.8$ and $\kappa \approx 10$ in which the full functionality of Eqs. (8b, 8c) is needed.

Similar arguments as above can be made for the functionality of $\kappa_{eff\_Ray}$ with the real part of the relative refractive index $n$. For small $n$ (i.e., $n \ll 1$ and $n \ll \kappa$), Eqs. (8b,c) can be approximated as

$$\kappa_{eff\_Ray}(m) \approx f_v n_m \frac{9\kappa}{(2-\kappa^2)^2} n = f_v \frac{9\kappa}{(2-\kappa^2)^2} n_0, \quad n \ll 1 \text{ and } n \ll \kappa, \tag{11}$$

corresponding to $\xi_{small\_n}(m) = \frac{9n}{(2-\kappa^2)^2}$.

For large $n$ (i.e., $n \gg 1$ and $n \gg \kappa$), Eqs. (8b, 8c) can be approximated as

$$\kappa_{eff\_Ray}(m) \approx 9 f_v n_m \kappa \, n^{-3} = 9 f_v \kappa_0 \, n^{-3}, \quad n \gg 1 \text{ and } n \gg \kappa, \tag{12}$$

corresponding to $\xi_{large\_n}(m) = \frac{9}{n^3}$.

Fig. 3 shows a log-log plot that demonstrates the functionality of

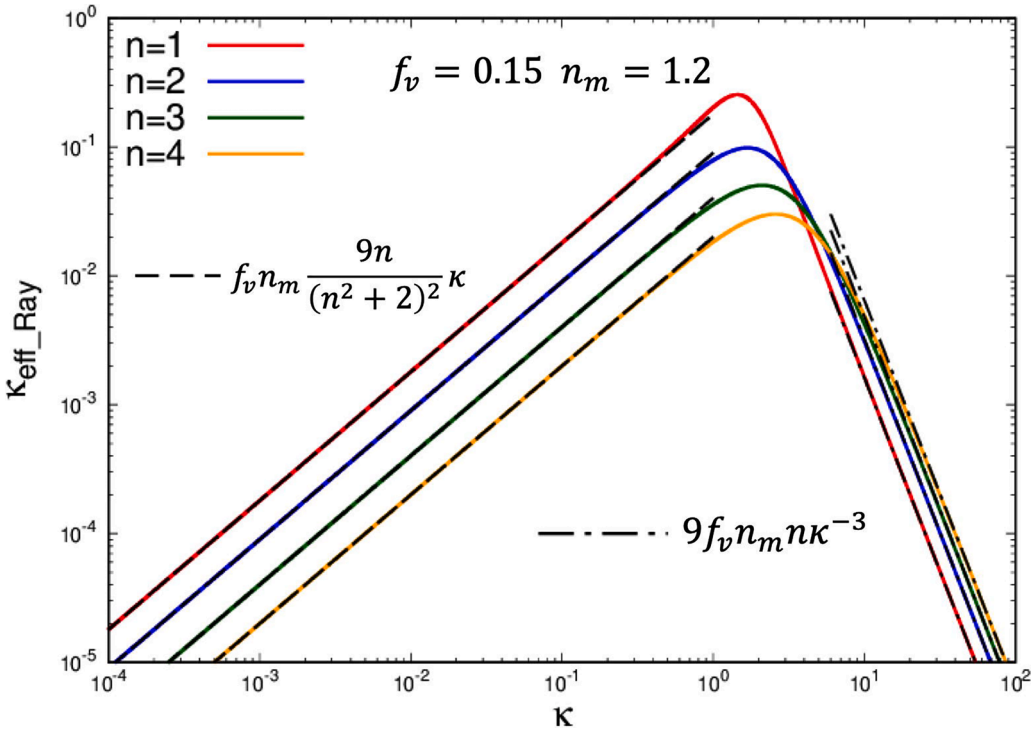


**Fig. 2.** Plot of $\kappa_{eff\_Ray}(m)$ for set real parts of the relative refractive index of the particles $n = 1, 2, 3, 4$ with a refractive index of the medium of $n_m = 1.2$ and volume fraction of $f_v = 0.15$, as a function of the relative imaginary part $\kappa$ of the refractive index of the particles.

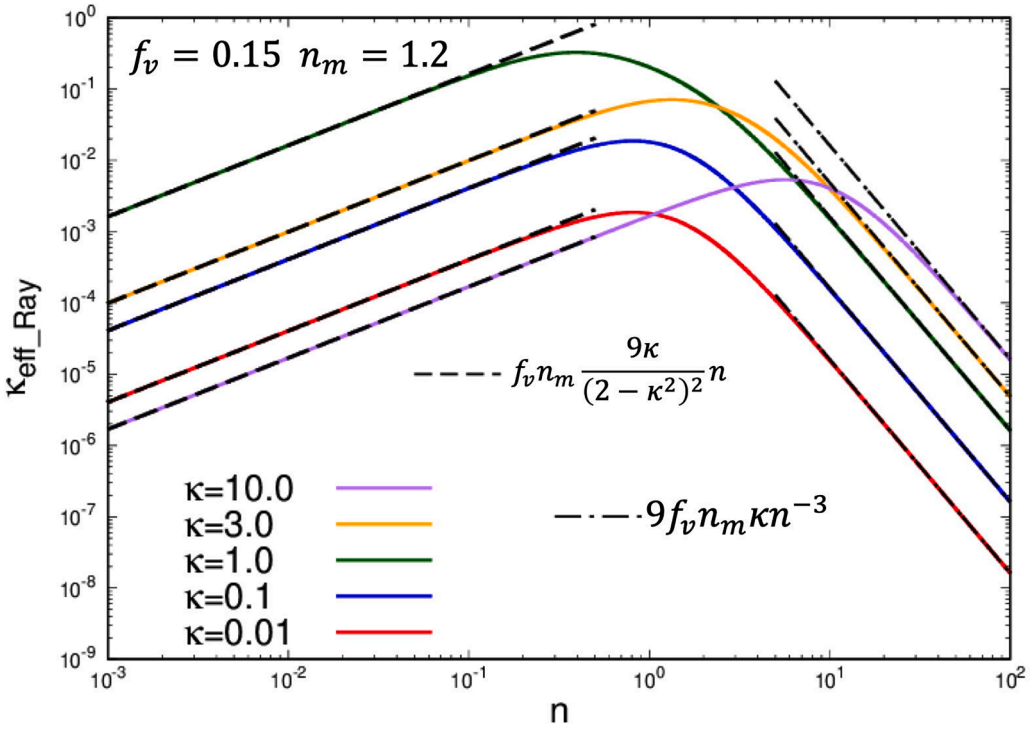


**Fig. 3.** Log-Log plot of $\kappa_{eff\_Ray}(m)$ for set imaginary parts of the relative refractive index of the particles $\kappa = 0.01, 0.1, 1.0, 3.0, 10.0$ with a refractive index of the medium of $n_m = 1.2$ and volume fraction of $f_v = 0.15$, as a function of the relative real part of the refractive index of the particles.

$\kappa_{eff\_Ray}$ as a function of the real part of the relative refractive index $n$, for set values of the imaginary part $\kappa = 0.01, 0.1, 1.0, 3.0,$ and10.0, essentially log-log x-y plots along five horizontal lines (for the five set values of $\kappa$) through a contour plot like the one shown in Fig. 1. In Fig. 3, the large and small $n$ behaviour described by Eq. (11) and Eq. (12) can been seen, as well a cross over region like that found in Fig. 2. The cross over region in Fig. 3 contains the range of the most common real parts of the relative refractive index $0.5 \lesssim n \lesssim 5.0$; therefore, the full functionality of Eqs. (8b, 8c) is generally needed.

Fig. 4a shows $\kappa_{eff\_Ray}$ as function of the real part of the relative refractive index $n$, for $\kappa = 0.01, 0.1, 1$ on a log-linear plot over this range and it can be seen that when $\kappa \lesssim 1$, $\kappa_{eff\_Ray}$ approximately follows an exponential functionality in the region $1.0 \lesssim n \lesssim 4.5$ given by

$$\kappa_{eff\_Ray}(m) \approx \frac{9}{4} f_v n_m \kappa e^{-\frac{3}{4}n} = \frac{9}{4} f_v \kappa_0 e^{-\frac{3}{4}n}, \quad 1.0 \lesssim n \lesssim 4.5. \tag{13}$$

However, as $\kappa$ increases past unity, Fig 4b demonstrates that the functionality of $\kappa_{eff\_Ray}$ in the range $1.0 \lesssim n \lesssim 4.5$ transitions back to that of Eq. (11). This is not due to $n$ being much less than unity, but to $\kappa$ becoming large compared to $n$.

### 3.1. Use of Rayleigh mixing rule to determine the imaginary refractive index of spherical particle ensembles

Dispersing an ensemble of spherical, homogeneous Rayleigh regime particles into a non-absorbing liquid with known refractive index $n_m$ and measuring the bulk absorption coefficient $\beta_{abs}$ of the resulting colloid can be used to determine the imaginary part of the particles. With a measured $\beta_{abs}$ the $\kappa_{eff\_Ray}$ of the colloid can be determined using Eq. (8a), followed by an inversion process to determine the imaginary part of the relative refractive index κ for the Rayleigh particles and thus $\kappa_0 = \kappa n_m$,

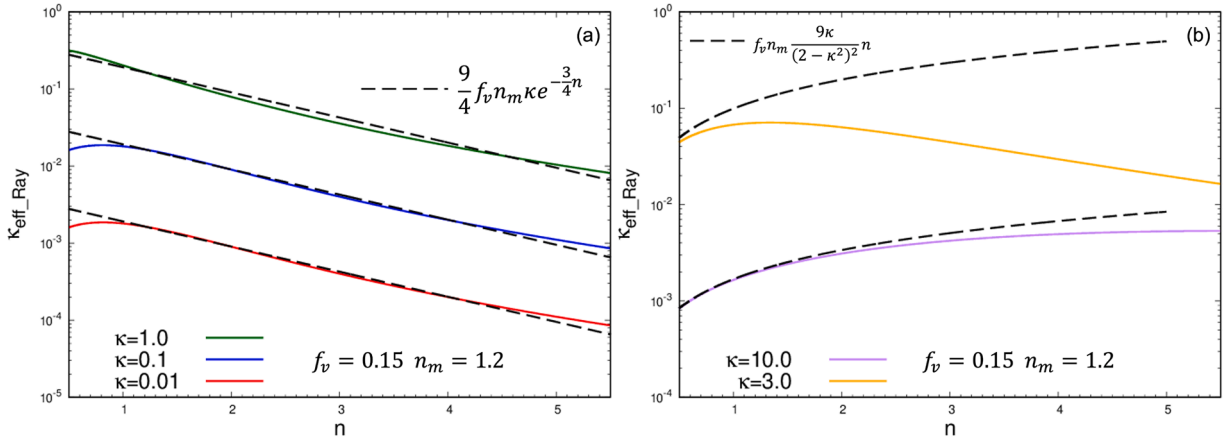


**Fig. 4.** (a) Log-linear plot of $\kappa_{eff\_Ray}(m)$ for set imaginary parts of the relative refractive index of the particles $\kappa = 0.01, 0.1, 1.0$ as a function of the relative real part of the refractive index of the particles. (b) Log-linear plot of $\kappa_{eff\_Ray}(m)$ for set imaginary parts of the relative refractive index of the particles $\kappa = 3.0, 10.0$ as a function of the relative real part of the refractive index of the particles.

the imaginary part of the Rayleigh particles refractive index. Such a measurement of the colloid's bulk absorption coefficient can be straightforward in the Rayleigh regime because then the extinction is nearly equal to the absorption. For example, for sufficiently small, absorbing particles in the Rayleigh regime the single scattering albedo, $SSA \sim x^3$ [10]. Once this is established, the absorption spectrum of the colloid can readily be determined with a spectrophotometer to yield the spectrum of the imaginary part of the refractive index of the particle material.

To obtain the imaginary part of the particle refractive index $\kappa_0$, Eqs. (8b or 8d) can be solved analytically to yield expressions for $\kappa$ and $\kappa_0$. Because these expressions are quite lengthy, this is best done using symbolic computation. Here we used Mathematica [23] yielding four analytical solutions for $\kappa = \kappa_0/n_m$, two of which are real and positive with physical meaning. The Mathematica notebook, complete with analytical solutions, is included in the Appendix.

A more intuitive approach examines Figs. 1 and 2 noticing that each value of $\kappa_{eff\_Ray}$ has two positive solutions for $\kappa$ and $\kappa_0$ because absorption increases proportionally to $\kappa$ for small $\kappa$ (see Eq. 9 and Fig. 2), then peaks in the cross over regime (Fig. 2), followed by absorption decreasing proportional to $\kappa^{-3}$ for large $\kappa$ (i.e., $\kappa \gg 1$) once particles become metallic and light only poorly penetrates them with the skin depth becoming smaller than the particle size [10,24]. Similarly, Fig. 3 shows there are also two $n$ values for each $\kappa_{eff\_Ray}$.

Therefore, to determine the imaginary part of particle refractive index of spherical particles in the Rayleigh regime from absorption measurements, the following conditions need to be fulfilled:

1. The refractive index of the non-absorbing liquid used for particle suspension must be known;
2. The absorbing particles must be small enough to be in the Rayleigh regime with $x \ll 1 and \kappa x \ll 1$ resulting in $SSA \ll 1$ and consequently negligible scattering [10];
3. The real part of the particle refractive index must be known reasonably well;
4. The imaginary part of the particle refractive index must be known well enough to know which of the two solutions (see Fig. 2) should be used.

Fulfilling some of these conditions is fairly easy while other ones pose some interesting challenges:

1. Refractive indices of non-absorbing pure and binary liquids are generally well known [25,26];
2. *SSA* and consequently the scattering contribution to extinction can be estimated and reduced, if needed, by using smaller particles [10];
3. The real part of the particle refractive index must be known well enough to achieve the desired accuracy for the imaginary part with a detailed sensitivity analysis to be included in an upcoming manuscript [27]. If this is not the case, matching of the real parts of the liquid and the particle enables determination of this particle property and, at the same time, minimization of particle scattering (beneficial for (2));
4. The existence of two analytical solutions will generally only be a problem in the cross over regime near the absorption peak (Fig. 2); however, most particle materials have an imaginary part of the refractive index $\kappa$ well below this peak with the possible exceptions of black carbon and hematite.

While some of these challenges are relatively straightforward, most of them require detailed analysis to estimate resulting measurement errors and potential improvements. This will be discussed in detail in an upcoming manuscript [27], but is outside of the scope of this paper.

### 3.2. Use of Rayleigh mixing rule for non-spherical particles

Particle polarizability depends on particle shape and that of non-spherical particles is different from that of spherical particles as used above. In Fig. 5, we explore the influence of particle shape on the Rayleigh absorption cross-section $C_{abs\_Ray}$ by plotting the ratio of this absorption cross-section for spheroids and for spheres for a few typical refractive indices (i.e, $n = 1.3$, 1.5 and $\kappa = 0.1$, 1.0) and aspect ratios ranging from 0.1 (oblate spheroid), 1.0 (sphere), to 10 (prolate spheroid) with analytical solutions taken from van de Hulst [11] and not repeated here. Curves with legend labelled with "$\kappa \leq 0.1$" represent all curves with$0 < \kappa \leq 0.1$, because these curves would be visually indiscernible in Fig. 5 with maximum differences of ~0.1%. Note that the shape dependence for moderately aspect ratios between 0.5 and 2.0 is generally less than ~5% with somewhat larger discrepancies of less than ~10% for aspect ratios near 0.5 and $n = 1.5$, $\kappa = 1.0$. Aspect ratios for atmospheric aerosols often have median values between 1.0 and 1.5 for urban regions [28], and of ~2.0 for mineral dust after long-range transport [29]. Therefore, it may be possible to ignore the often moderate (~5%) shape dependence of absorption cross section for atmospheric aerosols. However, examination of particle shapes and sizes with electron microscopy is recommended before using the Rayleigh mixing rule for a particular aerosols type.

## 4. Comparison with some other mixing rules

Here, we compare the effective imaginary part of the refractive index $\kappa_{eff\_i}$ of the composite medium calculated with different mixing rules $i$ with $\kappa_{eff\_Ray}$ calculated with the Rayleigh mixing rule Eq. (8b) by calculating the ratio $r_i$ as

$$r_i(m) = \frac{\kappa_{eff\_i}}{\kappa_{eff\_Ray}} \tag{14}$$

for the following mixing rules:

1. $i = Vol$: Refractive Index Volume Mixing Rule
2. $i = MG$: Maxwell Garnett Mixing Rule
3. $i = B$: Bruggeman Mixing Rule

For these mixing rules, we show the ratios $r_i$ in contour plots in the complex refractive index plane. In the case that $r_i$ has a dependence on the volume fraction, we will consider, $f_v = 0.1$, 0.15, 0.2, 0.3.

### 4.1. Refractive index volume mixing rule

Our result for the Rayleigh mixing rule Eq. (8b) is quite similar to the expression for $\kappa_{eff\_Vol}$, given by the imaginary refractive index volume mixing rule for a non-absorbing medium as [1]

$$\kappa_{eff\_Vol}(m) = \frac{V_{tp}}{V}\kappa_0 = f_v n_m \kappa. \tag{15a}$$

The difference between Rayleigh mixing rule Eq. (8b) and the volume mixing rule is the appearance of the factor $\xi(m)$ in Eq. (8b) this gives the ratio $r_{Vol}$ as

$$r_{Vol}(m) = \frac{1}{\xi(m)}. \tag{15b}$$

Fig. 5 shows a contour plot of the function $r_{vol}(m)$ as a function of the real and imaginary parts of the refractive index of the particle in the medium, $n$ and $\kappa$, respectively. The range of the real and imaginary parts in Fig. 6. are $1 \leq n \leq 4$ and $0 \leq \kappa \leq 3$. Within this range the maximum value of $r_{vol}$ is $r_{vol,max}$ $(n = 4, \kappa = 3) = 18.25$, and the minimum value of $r_{vol}$ is $r_{vol,min}$ $(n = 1, \kappa = 1) = 0.889$. Note that with the volume mixing rule Eq. (15a), the effective imaginary part of the refractive index of the bulk medium $\kappa_{eff\_Vol}$ can be calculated simply as the product of particle

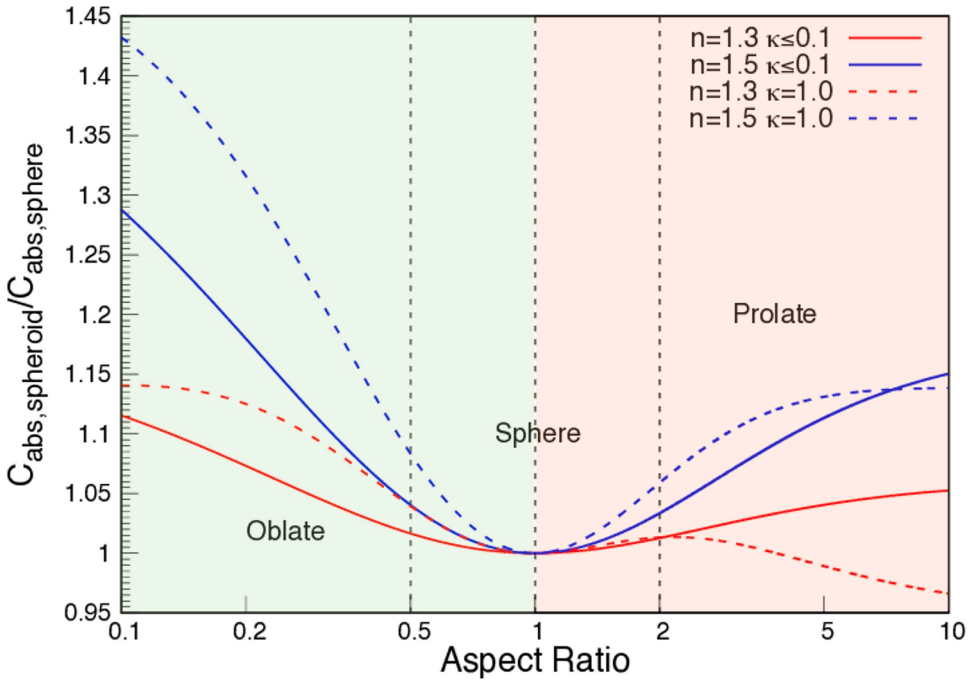


**Fig. 5.** Ratio of absorption cross-section $C_{abs\_Ray}$ of spheroids and that of spheres as function of spheroid aspect ratio. Curves with legend labelled with "$\kappa \leq 0.1$" represent all curves with$0 < \kappa \leq 0.1$.

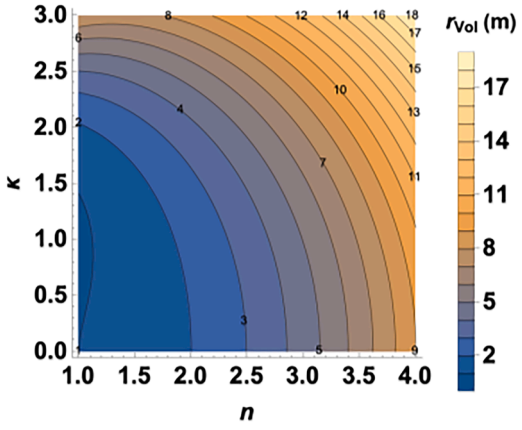


**Fig. 6.** Contour plot of the function $r_{vol}(m)$ as function of the real and imaginary parts of the refractive index of the particle in the medium, $n$ and $\kappa$, respectively.

fractional volume $f_v$, the non-absorbing medium's refractive index $n_m$, and the imaginary part of the refractive index $\kappa$ of the particle material and inversely, $\kappa$ can be determined simply from a measurement of the absorption and consequently imaginary part of refractive index of the composite medium. In contrast, for the exact Rayleigh solution Eq. (8b), the knowledge of the real part of the particle refractive index is also needed.

### 4.2. Maxwell Garnett mixing rule

Chýlek et al. [1] give the effective complex refractive index according to the Maxwell Garnett mixing rules as

$$m^2_{eff\_MG}(m) = n^2_m \frac{m_0^2 + 2n_m^2 + 2f_v\left(m_0^2 - n_m^2\right)}{m_0^2 + 2n_m^2 - f_v\left(m_0^2 - n_m^2\right)}. \tag{16a}$$

A factor of $n_m^2$ can be factored out of each term in the denominator and numerator of Eq. (16a) leading to

$$m^2_{eff\_MG}(m) = n^2_m \frac{m^2 + 2 + 2f_v\left(m^2 - 1\right)}{m^2 + 2 - f_v\left(m^2 - 1\right)}. \tag{16b}$$

It follows from Eq. (16b) that the imaginary part of the refractive index given by the Maxwell Garnett mixing rule is given by

$$\kappa_{eff\_MG}(m) = n_m\ Im\left[\sqrt{\frac{m^2 + 2 + 2f_v(m^2 - 1)}{m^2 + 2 - f_v(m^2 - 1)}}\right]. \tag{17}$$

Eq. (17) can be calculated numerically or approximated by expanding Eq. (16b) in a Maclaurin series (i.e., a Taylor series expansion about $f_v = 0$) [30], which gives

$$m^2_{eff\_MG}(m) \approx n^2_m\left(1 + 3\frac{m^2 - 1}{m^2 + 2}f_v + 3\left(\frac{m^2 - 1}{m^2 + 2}\right)^2 f_v^2 \cdots\right). \tag{18}$$

Keeping the first two terms of Eq. 18 and solving for the imaginary part of $m_{eff\_MG}$ leads to

$$\kappa_{eff\_MG}(m) \approx n_m\ Im\left[\sqrt{1 + 3\frac{m^2 - 1}{m^2 + 2}f_v}\right]. \tag{19a}$$

The square root can be expanded into a Taylor series as $\sqrt{1+x} = 1 + \frac{1}{2}x - \frac{1}{8}x^2 + \ldots$

Neglecting quadratic and higher terms yields

$$\kappa_{eff\_MG}(m) \cong\ n_m\ Im\left[1 + \frac{3}{2}\frac{m^2 - 1}{m^2 + 2}f_v\right] = n_m\frac{3}{2}f_v\ Im\left[\frac{m^2 - 1}{m^2 + 2}\right]$$
$$= n_m f_v \kappa\ \xi(m). \tag{19b}$$

Comparing Eq. (8b) and Eq. (19b) it can be seen that the approximation of the Maxwell Garnett mixing rule for small particle volume fractions leads to the same $\kappa_{eff}$ as our Rayleigh mixing rule.

A ratio of Eq. (17) and Eq. (8b) leads to

$$r_{MG}(\mathrm{m}) = \frac{Im\left[\sqrt{\frac{m^2+2+2f_v(m^2-1)}{m^2+2-f_v(m^2-1)}}\right]}{f_v\kappa\ \xi(m)}, \tag{20}$$

which can be calculated numerically. Fig. 7 shows a contour plot of the function $r_{MG}(m)$ as a function of the real and imaginary parts of the refractive index of the particle, Fig. 6a, 6b, 6c, and 9d have a volume fraction of $f_v = 0.1, 0.15, 0.2, 0.3$, respectively. The range of the real and imaginary parts in Fig. 6 are $1 \le n \le 4$ and $0 \le \kappa \le 3$. Within this range, when the volume fraction is $f_v = 0.1$, the maximum value of $r_{MG}$ is $r_{MG,max}$ $(n = 1, \kappa = 2.61) = 1.094$, and the minimum value of $r_{MG}$ is $r_{MG,min}$ $(n = 1, \kappa = 0.007) = 1.0$. Fig. 7a demonstrates the small volume fraction approximations that lead to the agreement between Eq. (8b) and Eq. (19b). As the volume fraction increases, the deviations between the Maxwell Garnett mixing rule and the Rayleigh mixing rule increases, at a volume fraction of $f_v = 0.3$, the maximum value of $r_{MG}$ is $r_{MG,max}$ $(n = 1, \kappa = 2.72) = 1.526$, and the minimum value of $r_{MG}$ is $r_{MG,min}$ $(n = 1, \kappa = 0.5) = 1.0$. Even at a larger volume fraction of $f_v = 0.3$, within the range $1 \le n \le 2$ and $0 \le \kappa \le 1$, deviations between the Maxwell Garnett and Rayleigh mixing rules are still under 16%.

### 4.3. Bruggeman mixing rule

The Bruggeman mixing rule is similar to that of the Maxwell Garnett mixing rule, but has a symmetry not found in Maxwell Garnett. With the Bruggeman mixing rule no distinction is made between the medium and the inclusions [30], and is given by Chýleket al. [1] as

$$f_{v\_med}\frac{n_m^2 - m_{eff\_B}^2}{n_m^2 + 2m_{eff\_B}^2} + f_v\frac{m_0^2 - m_{eff\_B}^2}{m_0^2 + 2m_{eff\_B}^2} = 0, \tag{21}$$

where $f_{v\_med}$ is the fractional volume of the non-absorbing medium, and the condition $f_{v\_med} + f_v = 1$ is necessary. The symmetry of the Bruggeman mixing rule can be seen in Eq. (21), as the exchange of the medium and inclusion terms leads to the same equation. Eq. (21) can be solved for the Bruggeman effective refractive index leading to [30]

$$m_{eff\_B}^2(m) = n_m^2\frac{b + \sqrt{8m^2 + b^2}}{4}, \tag{22}$$

where $b$ is given by

$$b = (2f_{v\_med} - f_v) + (2f_v - f_{v\_med})m^2. \tag{23}$$

The imaginary part of the Bruggeman effective refractive index can be found by taking the imaginary part of the square root of Eq. (22) given by

$$\kappa_{eff\_B}(m) = n_m\ Im\left[\sqrt{\frac{b + \sqrt{8m^2 + b^2}}{4}}\right]. \tag{24}$$

The most straightforward way to arrive at a value for $\kappa_{eff\_B}$ in Eq. (24) is to calculate it numerically. However, when the volume fraction of the inclusions is $f_v \ll 1$, a Maclaurin series expansion can be used on Eq. (22) leading to

$$m_{eff\_B}^2(m) \approx n_m^2\left(1 + 3\frac{m^2 - 1}{m^2 + 2}f_v + 9m^2\frac{(m^2 - 1)^2}{(m^2 + 2)^3}f_v^2\cdots\right). \tag{25}$$

The first two terms of the expansion of the Bruggeman mixing rule are identical to that of the Maxwell Garnett found in Eq. 18, but the two mixing rules differ, when comparing the third term. As with the Maxwell Garnett, when $f_v \ll 1$ the third and higher order terms can be neglected in Eq. (25). Following the steps of the previous section leads to an identical expression as Eq. (8b), and Eq. (19b) for the Bruggeman mixing rule

$$\kappa_{eff\_B}(m) \cong n_m f_v \kappa\ \xi(m). \tag{26}$$

A ratio of Eq. (24) and Eq. (8b) leads to

$$r_B(\mathrm{m}) = \frac{Im\left[\sqrt{\frac{m^2+2+2f_v(m^2-1)}{m^2+2-f_v(m^2-1)}}\right]}{f_v\kappa\ \xi(m)}, \tag{27}$$

which can be calculated numerically. Fig. 8 shows a contour plot of the function $r_B(m)$ as a function of the real and imaginary parts of the refractive index of the particle, Fig. 8a, 8b, 8c, and 8d have a volume fraction of $f_v = 0.1, 0.15, 0.2, 0.3$ respectively. The range of the real and imaginary parts in Fig. 8 are $1 \le n \le 4$ and $0 \le \kappa \le 3$. Within this range, when the volume fraction is $f_v = 0.1$, the maximum value of $r_B$ is $r_{B,max}$ $(n$

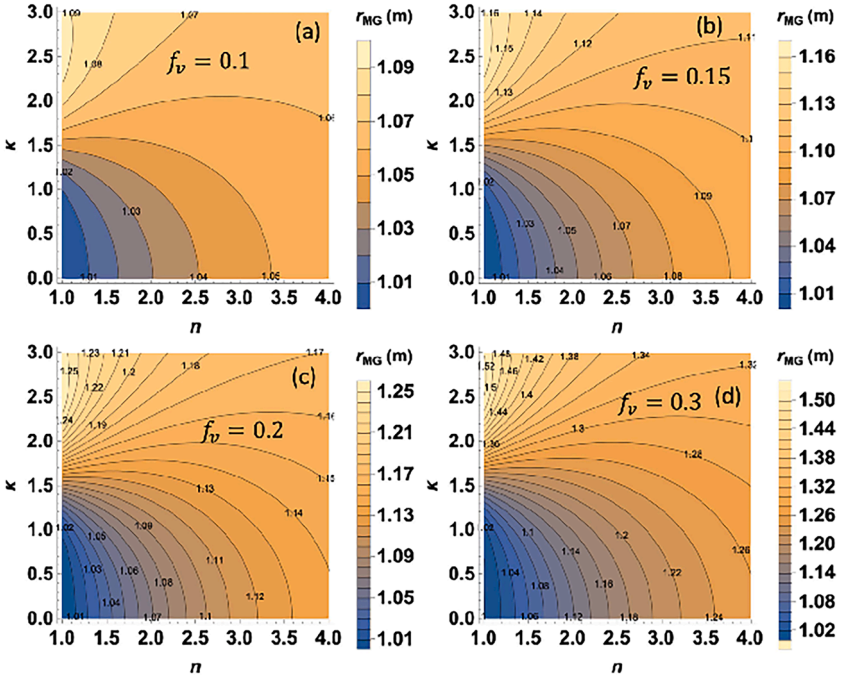


**Fig. 7.** Contour plot of the function $r_{MG}(m)$ as function of the real and imaginary parts of the refractive index of the particle in the medium, $n$ and $\kappa$, respectively. (a) The volume fraction is $f_v = 0.1$. (b) The volume fraction is $f_v = 0.15$. (c) The volume fraction is $f_v = 0.2$. (d) The volume fraction is $f_v = 0.3$.

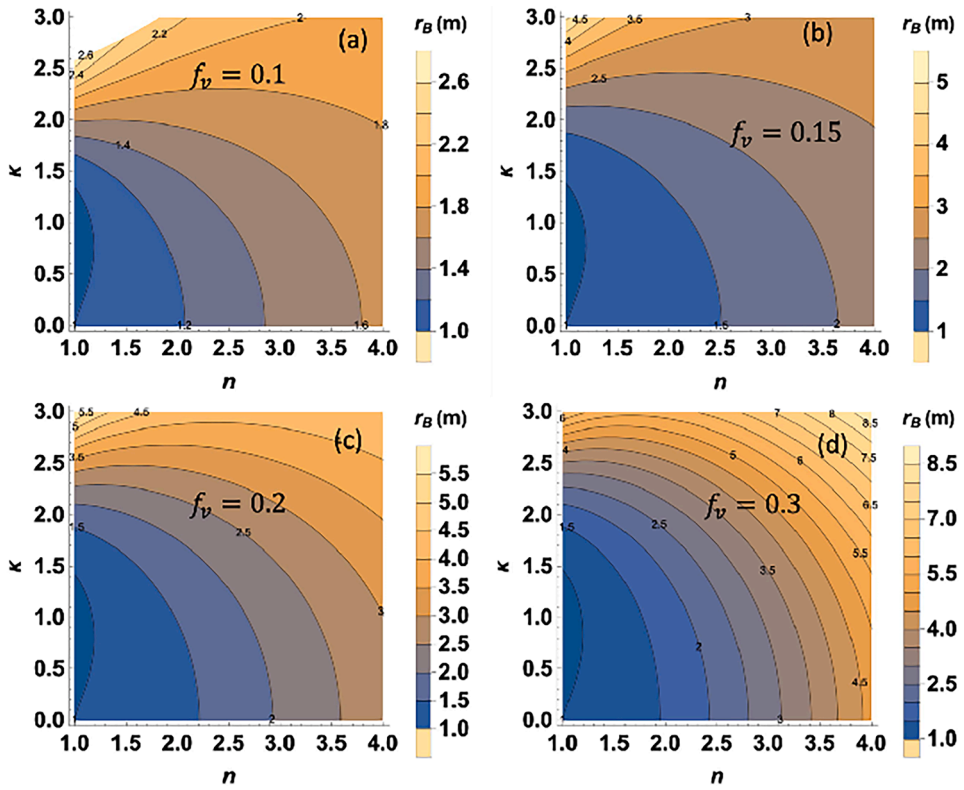


**Fig. 8.** Contour plot of the ratio $r_B(m)$ as function of the real and imaginary parts of the refractive index of the particle in the medium, $n$ and $\kappa$, respectively. (a) The volume fraction is $f_v = 0.1$. (b) The volume fraction is $f_v = 0.15$. (c) The volume fraction is $f_v = 0.2$. (d) The volume fraction is $f_v = 0.3$.

$= 1, .04\kappa = 2.61) = 2.69$, and the minimum value of $r_B$ is $r_{B,min}$ ($n = 1$, $\kappa = 1.006$) $= 0.95$. Fig. 8a demonstrates the small volume fraction approximations that lead to the agreement between Eq. (8b) and Eq. (26), but it also can be seen that the small volume fraction approximations that lead to Eq. (26) are not nearly as accurate when applied to the Bruggeman mixing rule. As the volume fraction increases, the deviations between the Bruggeman mixing rule and the Rayleigh mixing rule increase, at a volume fraction of $f_v = 0.3$, the maximum value of $r_B$ is $r_{B,max}$ ($n = 4$, $\kappa = 3$) $= 8.9$, and the minimum value of $r_B$ is $r_{B,min}$ ($n = 1$, $\kappa = 1.05$) $= 0.88$. The contour plot for $r_B$ in Fig. 8 show that there is a much greater dependence on both the real and imaginary parts of the refractive index of the particle for the Bruggeman mixing rule.

## 5. Conclusions

We have derived a Rayleigh mixing rule for composite media in a simple way with no additional assumptions from the Lorentz-Lorenz equations governing spherical particle optics in the Rayleigh regime. This mixing rule directly relates the effective imaginary part of the refractive index of a composite medium, such as an aerosol or colloid, to the complex refractive index of the suspended Rayleigh particles and the refractive index of the non-absorbing, surrounding medium. We further inverted this mixing rule toward determining the imaginary part of refractive index of the particles from an extinction measurement for the composite medium. This inversion generally yields two mathematical results and some a priori knowledge is needed to decide upon the appropriate solution.

Therefore, the Rayleigh mixing rule offers an opportunity to determine the imaginary part of refractive index spectra of Rayleigh particles, often only weakly dependent on their morphology from an extinction spectrum of the composite medium. For this, Rayleigh particles with a reasonably well-known real refractive index are suspended in a non-absorbing medium with known refractive index spectrum and the extinction spectrum is acquired with a spectroradiometer. Details and constraints of this use of the Rayleigh mixing rule will be presented elsewhere [27].

The Rayleigh mixing rule is compared with three widely used mixing rules (i.e., volume, Maxwell Garnett, and Bruggeman mixing rules) and we show that, in the small volume fraction regime, both the Maxwell Garnet and Bruggeman mixing rules agree with the Rayleigh mixing rule.

## Funding

This work was supported in part by the Department of Energy (DOE), Los Alamos National Laboratory (LANL) through Kansas State University (KSU) under Grant no. A23-0465-S001, by the National Science Foundation under grant Grant No. OIA- 2148788, and by NASA ROSES under grant 80NSSC20M0205 (PACE SAT Project: PACE UV ROAD).

## CRediT authorship contribution statement

**Hans Moosmüller:** Writing – review & editing, Writing – original draft, Visualization, Methodology, Investigation, Funding acquisition, Formal analysis, Conceptualization. **Justin B. Maughan:** Formal analysis, Investigation, Methodology, Visualization, Writing – original draft, Writing – review & editing. **Prakash Gautam:** Writing – review & editing, Investigation. **Christopher M. Sorensen:** Funding acquisition, Investigation, Methodology, Writing – review & editing.

## Declaration of competing interest

The authors declare that they have no known competing financial interests or personal relationships that could have appeared to influence the work reported in this paper.

## Supplementary materials

Supplementary material associated with this article can be found, in the online version, at doi:10.1016/j.jqsrt.2024.109254.

## Appendix

Mathematica Notebook including four analytical solutions of Eq. 8d for $\kappa = \kappa_0/n_m$,; two of these solutions are real and positive with physical meaning.

## Data availability

No data was used for the research described in the article.

## References


[1] Chýlek P, Srivastava V, Pinnick RG, Wang RT. Scattering of Electromagnetic Waves by Composite Spherical Particles: Experiment and Effective Medium Approximations. Appl Opt 1988;27:2396–404.
[2] Marston PL, Langley DS, Kingsbury DL. Light Scattering by Bubbles in Liquids: Mie Theory, Physical-Optics Approximations, and Experiments. Appl Sci Res. 1982;38:373–83.
[3] Mishchenko MI. Electromagnetic Scattering by Nonspherical Particles: A Tutorial Review. J Quant Spectrosc Radiat Transf 2009;110:808–32.
[4] Saito M, Yang P. Generalization of Atmospheric Nonspherical Particle Size: Interconversions of Size Distributions and Optical Equivalence. J Atmos Sci 2022;79:3333–49.
[5] Penndorf R. Tables of the Refractive Index for Standard Air and the Rayleigh Scattering Coefficient for the Spectral Region between 0.2 and 20.0 μm and Their Application to Atmospheric Optics. J Opt Soc Am 1957;47:176–82.
[6] Hale GM, Querry MR. Optical Constants of Water in the 200-nm to 200-μm Wavelength Region. Appl Opt 1973;12:555–63.
[7] Laskar JM, Shravan Kumar P, Herminghaus S, Daniels KE, Schröter M. High Refractive Index Immersion Liquid for Superresolution 3D Imaging Using Sapphire-Based Aplanatic Numerical Aperture Increasing Lens Optics. Appl Opt 2016;55:3165–9.
[8] Bohren CF, Huffman DR. Absorption and scattering of light by small particles. New York: Wiley; 1998.
[9] Moosmüller H, Arnott WP. Particle Optics in the Rayleigh Regime. J Air Waste Manage Assoc 2009;59:1028–31.
[10] Moosmüller H, Sorensen CM. Small and Large Particle Limits of Single Scattering Albedo for Homogeneous, Spherical Particles. J Quant Spectrosc Radiat Transf 2018;204:250–5.
[11] van de Hulst HC. Light scattering by small particles. New York: Dover Publications; 1981.
[12] Mie G. Beiträge zur Optik trüber Medien, speziell kolloidaler Metallösungen. Ann Phys 1908;330:377–445.
[13] Lorentz HA. Ueber die Beziehung zwischen der Fortpflanzungsgeschwindigkeit des Lichtes und der Körperdichte. Ann Phys 1880;245:641–65.
[14] Lorenz L. Ueber die Refractionsconstante. Ann Phys 1880;247:70–103.
[15] Sorensen CM. Light Scattering by Fractal Aggregates: A Review. Aerosol Sci Technol 2001;35:648–87.
[16] Sorensen CM. Light scattering and absorption by particles. IOP Publishing; 2022.
[17] Moosmüller H, Chakrabarty RK, Ehlers KM, Arnott WP. Absorption Ångström Coefficient, Brown Carbon, and Aerosols: Basic Concepts, Bulk Matter, and Spherical Particles. Atmos Chem Phys 2011;11:1217–25.
[18] Sun HL, Biedermann L, Bond TC. Color of Brown Carbon: A Model for Ultraviolet and Visible Light Absorption by Organic Carbon Aerosol. Geophys Res Lett 2007;34. https://doi.org/10.1029/2007GL029797.
[19] Moosmüller H, Chakrabarty RK, Arnott WP. Aerosol Light Absorption and its Measurement: A Review. J Quant Spectrosc Radiat Transf 2009;110:844–78.
[20] Wang G, Chakrabarti A, Sorensen CM. Effect of the Imaginary Part of the Refractive Index on Light Scattering by Spheres. J Opt Soc Am A 2015;32:1231–5.
[21] Moosmüller H. Chapter 16 - Optical Properties of Nonspherical, Light-Absorbing Particles: Black Carbon and Mineral Dust Aerosols. In: Mengüç MP, Francoeur M, editors. Light, plasmonics and particles. 1st ed. Elsevier Science and Technology Publishing; 2023. p. 349–69.
[22] Castellanos P, Colarco P, Espinosa WR, Guzewich SD, Levy RC, Miller RL, et al. Mineral Dust Optical Properties for Remote Sensing and Global Modeling: A Review. Remote Sens Environ 2024;303:113982.
[23] Wolfram Research Inc. Mathematica. Champaign, Illinois: Wolfram Research, Inc.; 2021.
[24] Sorensen CM, Maughan JB, Moosmüller H. Spherical Particle Absorption over a Broad Range of Imaginary Refractive Index. J Quant Spectrosc Radiat Transfer 2019;226:81–6.
[25] Reis JCR, Lampreia IMS, Santos ÂFS, Moita MLCJ, Douhéret G. Refractive Index of Liquid Mixtures: Theory and Experiment. ChemPhysChem 2010;11:3722–33.
[26] Pretorius F, Focke WW, Androsch R, du Toit E. Estimating Binary Liquid Composition from Density and Refractive Index Measurements: A Comprehensive Review of Mixing Rules. J Mol Liq 2021;332:115893.
[27] Maughan JB, Moosmüller H, Gautam P, Sorensen CM. Retrieval of Complex Refractive Index Spectra Using Colloids in the Rayleigh Regime: Theory. J Quant Spectrosc Radiat Transfer 2024. in preparation.
[28] Pipal AS, Kaur P, Singh SP, Rohra H, Morphology Taneja A. Aspect Ratio, and Surface Elemental Composition of Primary Aerosol Particles at Urban Region of India. Environ Sci Pollut Res 2024;31:47946–59.
[29] Reid EA, Reid JS, Meier MM, Dunlap MR, Cliff SS, Broumas A, et al. Characterization of African Dust Transported to Puerto Rico by Individual Particle and Size Segregated Bulk Analysis. J Geophys Res 2003;108.
[30] Markel VA. Introduction to the Maxwell Garnett Approximation: Tutorial. J Opt Soc Am A 2016;33:1244–56.